Connection between modeled blackbody radiation and dipole emission in large-area nanostructures

Anttu, Nicklas

Published in:
Optics Letters

DOI:
10.1364/OL.41.001494

2016

Document Version:
Peer reviewed version (aka post-print)

Connection between modeled blackbody radiation and dipole emission in large-area nanostructures

Author: N. Anttu

Optics Letters Vol. 41, Issue 7, pp. 1494-1497 (2016), https://doi.org/10.1364/OL.41.001494

Connection between modeled blackbody radiation and dipole emission in large-area nanostructures

NICKLAS ANTTU[1,*]

[1] *Division of Solid State Physics and NanoLund, Lund University, Box 118, 22100 Lund, Sweden*
**Corresponding author: nicklas.anttu@ftf.lth.se*

Received XX Month XXXX; revised XX Month, XXXX; accepted XX Month XXXX; posted XX Month XXXX (Doc. ID XXXXX); published XX Month XXXX

When modeling the emission of light from nanostructures, we typically study either (1) blackbody radiation or (2) dipole emission. For effective analysis, it is important to know how results from these two types of modeling are related. Here, we use the Kirchoff's reciprocity to study how interference affects the emissivity and number of emitted blackbody photons from a thin film for varying thickness. Next, we use the Lorentz' reciprocity to study how interference modifies the emission rate of a dipole placed within the same film. Finally, to find the connection between these two emission types, we use the Kirchoff's and Lorentz' reciprocity simultaneously for an arbitrary three dimensional large-area nanostructure. We show analytically how the blackbody radiation can be represented as the integrated emission from homogeneously distributed dipoles in the nanostructure. In this case, the dipole moment density is determined by the refractive index of the nanostructure.

OCIS codes: *(310.6628) Subwavelength structures, nanostructures; (300.2140) Emission; (230.3670) Light-emitting diodes.*

http://dx.doi.org/10.1364/OL.99.099999

The understanding of the emission of light is important for the analysis of many opto-electronics applications. For example, for solar cells, the voltage dependent emission of photons sets an upper limit on the open-circuit voltage and consecutively on the power output and efficiency [1-7]. For light emitting diodes (LEDs) in turn, the emission rate of photons dictates the fraction of recombination that goes through radiative and non-radiative channels, therefore affecting the efficiency of the LED [8-11].

The emission of light from nanostructures is often modeled either as blackbody radiation or as dipole emission. It is therefore important to know how the results obtained with these two different analysis methods are related.

When considering blackbody radiation, the geometry of the nanostructure affects the emissivity, which relates the emission of the nanostructure to that of a perfect blackbody [5, 12]. When considering the emission of light from a dipole inside the nanostructure, the interference of light in the nanostructure affects instead the emission rate and the re-absorption of photons. The blackbody radiation shows an explicit n^2 dependence of the refractive index of the surrounding medium [12]. In contrast, the dipole emission shows a dependence of n to the first power [13]. However at a fundamental level, the blackbody radiation should originate from emission within the structure. For example, the blackbody radiation can be analyzed in terms of the correlation of randomly fluctuating current sources placed inside the nanostructure [14]. However, in the dipole emission modeling we consider here, the dipole source does not fluctuate.

Here, to bring clarity to the connection between the modeling of blackbody radiation and this modeling of the dipole emission, we study theoretically the modified emission of light from a simple nanostructure model system, the planar thin film. We vary the film thickness and study the emission of photons from the top and the bottom side of the film. To study the blackbody radiation, we employ Kirchoff's reciprocity, which relates the absorptance of the structure to the emissivity. To study the dipole emission, we use the Lorentz' reciprocity, which relates the enhancement of incident light to the enhancement of the emission rate.

Finally, by combining Kirchoff's and Lorentz' reciprocity, we show analytically for an arbitrary three-dimensional nanostructure the connection between these two emission types. The blackbody radiation is formally equivalent to the emission from homogeneously distributed dipoles in the nanostructure.

We consider a thin-film system of thickness L and refractive index n_{film}. The film is placed between two semi-infinite regions of refractive index n_{top} above and n_{bot} below (Fig. 1(a)). We concentrate on the wavelength λ = 900 nm, but our conclusions apply for other wavelengths also. We use for the thin-film a refractive index of n_{film} = 3.5 + i0.1 where the non-zero imaginary part induces absorption of light.

We define the emission angles θ_{top} and θ_{bot} relative to the surface normal of the top and bottom interface, respectively. Due to the symmetry through rotation by an angle φ around the z axis, this thin-film system does not show a dependence on the azimuth angles φ_{top} and φ_{bot}. We denote by TM (TE) polarized light such light that has (doesn't have) an electric field component in the propagation plane (see Fig. 1(a)).

Any structure emits light at thermal equilibrium as blackbody radiation [12]. The emissivity e of the system describes how well the system emits compared to a perfectly emitting blackbody with $e = 1$. For the thin-film system in Fig. 1(a), we consider explicitly the emissivity $e_{top,TE(TM)}(\theta_{top})$ and $e_{bot,TE(TM)}(\theta_{bot})$ of TE and TM polarized light to the top and the bottom side at angles θ_{top} and θ_{bot}, respectively.

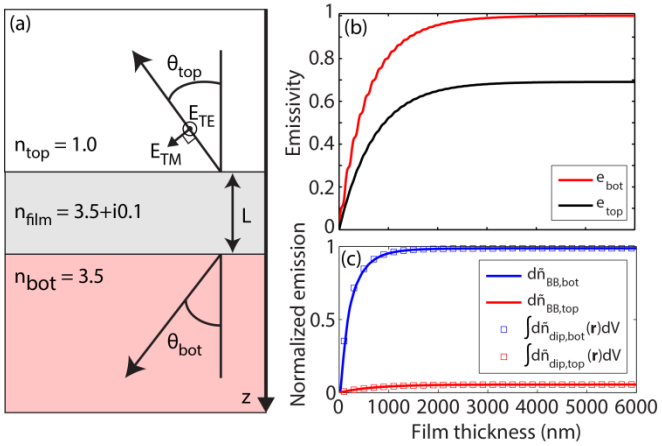

Fig. 1. (a) Schematic of a thin film of thickness L and refractive index n_{film}. The semi-infinite region on top of the film is of refractive index n_{top} and the region at the bottom of n_{bot}. (b) The emissivity e_{top} and e_{bot} to the top and bottom side for $\theta_{top} = 0$ and $\theta_{bot} = 0$ for varying thickness $0 < L < 6000$ nm of the thin film. Notice that for $\theta_{top} = 0$ and $\theta_{bot} = 0$, there is no polarization dependence of the emission in this thin-film system. (c) Blackbody emission rate $d\tilde{n}_{BB,top}$ and $d\tilde{n}_{BB,bot}$ of the thin film in (a) to, respectively, the top $n_{top} = 1.0$ side and the bottom $n_{bot} = 3.5$ side, according to Eq. (1). The results are normalized to $d\tilde{n}_{BB,n3.5}$, the blackbody radiation of a perfect blackbody into a surrounding $n = 3.5$ refractive index medium. Here, we show also the corresponding dipole emission [Eq. (2)]. For this dipole emission, we chose $P_{dip} = P_{dip,gen}$ according to Eq. (9) to yield equivalency with the blackbody radiation after integration over the thin film volume

A convenient way to analyze the emissivity of a structure is to use Kirchoff's reciprocity which relates the emissivity of a structure to the absorptance $A(\lambda)$ of the structure through $A(\lambda) = e(\lambda)$ [12]. Here, $A(\lambda)$ is the fraction of incoming photons that the structure absorbs at wavelength λ (note that we drop, unless otherwise marked, the explicit dependence on λ in the rest of the paper to simplify the notation). This reciprocity originates from the requirement that the system should at thermal equilibrium absorb as many of the incoming blackbody photons from the surrounding as it emits into the surrounding. The reciprocity holds separately for each incidence angle and polarization. That is, $e_{top,TE(TM)}(\theta_{top}) = A_{top,TE(TM)}(\theta_{top})$ and $e_{bot,TE(TM)}(\theta_{bot}) = A_{bot,TE(TM)}(\theta_{bot})$ [2, 3].

In our numerical optics modeling, we use a scattering matrix method [15], which solves the Maxwell equations for a given geometry of the system and for given refractive indexes of the constituent materials. In this way, we take into account the interference of light reflected at the two interfaces of the thin film, including multiple scattering of light between the interfaces. We perform the simulation for light incident either from the top or the bottom side and calculate $A_{top,TE(TM)}(\theta_{top})$ and $A_{bot,TE(TM)}(\theta_{bot})$ to obtain the information needed for the emission analysis.

We show in Fig. 1(b) the emissivity of the thin film at $\theta_{top} = 0$ and $\theta_{bot} = 0$, respectively. First, we see that both e_{top} and e_{bot} go toward zero when $L \to 0$. Thanks to the Kirchoff's reciprocity of $e = A$, we can understand this dependence on L from the expected behavior of the absorption of light: A film of decreasing thickness is expected to absorb less and less light so that $e = A \to 0$ as $L \to 0$.

Next, we find slight oscillations in e_{bot} as L increases. Also this behavior can be understood from the analysis of the absorptance A. The oscillations originate from the L dependent interference between the incident light propagating toward the top side and the light reflected back from the top interface toward the bottom side. No such oscillations are visible in e_{top} in Fig. 1(b). To understand this difference, we study the reflection at the top and at the bottom interface. The reflection at the top interface for $\theta_{top} = 0$ is given from the Fresnel equations as $R_{top} = |n_{film} - n_{top}|^2 / |n_{film} + n_{top}|^2 \approx 0.31$, which is large enough to give noticeable contribution to $A_{bot} = e_{bot}$. In contrast, the reflection at the bottom interface for $\theta_{top} = 0$ shows a low value of $R_{bot} = |n_{film} - n_{bot}|^2 / |n_{film} + n_{bot}|^2 \approx 0.0002$. Thus, for $\theta_{top} = 0$, the reflection of light from the bottom interface is expected to give a negligible contribution to $A_{top} = e_{top}$.

Lastly, we see in Fig. 1(b) that both e_{top} and e_{bot} saturate for large L. Here, all the light that can couple into the thin film is absorbed. Therefore, R_{top} and R_{bot} limit the absorption and consecutively the emissivity. Indeed, we find in Fig. 1(b) the limiting values of $e_{top} = A_{top} \to 1 - R_{top} \approx 0.69$ and $e_{bot} = A_{bot} \to 1 - R_{bot} \approx 1$ when $L \to \infty$.

Note that for this thin film system, we expect for $\theta_{top} > 0$ and $\theta_{bot} > 0$ a faster convergence of the emissivity toward the corresponding reflection-limited values at large L since the light propagates effectively a longer distance inside the thin film. Thus, for $L > 6000$ nm, we do not expect to see in the emission properties any longer a dependence on the film thickness.

Next, we calculate $d\tilde{n}$, the rate of emitted blackbody photons to the top and to the bottom side in a wavelength range $d\lambda$ centered around the wavelength λ, per unit area of thin film [2, 3, 12]:

$$d\tilde{n}_{BB,TE(TM),top(bot)} = 2\pi \frac{c n_{top(bot)}^2}{\lambda^4 \left[\exp(\hbar 2\pi c / (\lambda k_B T)) - 1\right]} d\lambda \times \int_0^{\pi/2} A_{top(bot),TE(TM)}(\theta_{top(bot)}) \cos(\theta_{top(bot)}) \sin(\theta_{top(bot)}) d\theta_{top(bot)}. \quad \textbf{(1)}$$

Here, the factor $\sin(\theta_{top(bot)})$ arises from the integration over the solid angle. In contrast, the $\cos(\theta_{top(bot)})$ factor arises from the properties of blackbody radiation [12]. Note that we use the tilde to discriminate $d\tilde{n}$ from n, the refractive index.

For easy presentation, we show the polarization summed response $d\tilde{n}_{BB,top(bot)} = (d\tilde{n}_{BB,TE,top(bot)} + d\tilde{n}_{BB,TM,top(bot)})$. Also, we normalize the results to $d\tilde{n}_{BB,n3.5}$, the polarization summed emission from a perfectly absorbing black body into an $n = 3.5$ medium. Explicitly, $d\tilde{n}_{n3.5BB}$ is calculated with $A_{TE(TM),bot} = 1$ in Eq. (1).

The emission to the top and the bottom side saturates for $L > 3000$ nm, which orginates from a saturation of the $\theta_{top(bot)}$ averaged $e_{top(bot)}\cos(\theta_{top(bot)})\sin(\theta_{top(bot)}) = A_{top(bot)}\cos(\theta_{top(bot)})\sin(\theta_{top(bot)})$ with increasing L. The emission to the bottom side saturates for large L to a reflection-limited value very close to that of the perfectly absorbing black body, corresponding to a normalized value of 1 in Fig. 1(b). Therefore, the θ_{bot} averaged $R_{bot}(\theta_{bot})\cos(\theta_{bot})\sin(\theta_{bot})$ shows very low values, as could be expected from the small difference between $n_{bot} = 3.5$ and $n_{film} = 3.5 + i0.1$.

Furthermore, from Eq. (1), we would expect a $n_{bot}^2 / n_{top}^2 = 3.5^2 / 1^2 = 12.25$ times lower emission into the top side at large L if both sides have a perfect anti-reflection coating with $R = 0$ (so that at large L, the reflectance-limited emission is given by $e = A = 1 - R \to$

1). However, from Fig. 1(b) we find instead a difference by a factor of 17.9 between $d\tilde{n}_{bot}$ and $d\tilde{n}_{top}$ at large L. Since the θ_{bot} averaged $R_{bot}(\theta_{bot})\cos(\theta_{bot})\sin(\theta_{bot})$ is low, we conclude that the θ_{top} averaged $R_{top}(\theta_{top})\cos(\theta_{top})\sin(\theta_{top})$ leads to a drop of 1 - 12.25 / 17.9 ≈ 32 % in the number of emitted photons.

Above, we considered the blackbody emission from the thin film. In that analysis, the emissivity of the film was modulated by the film thickness. Now we turn to look at dipole emission from a well-defined location inside the thin film. Note that we consider a material with an isotropic refractive index through the choice n_{film} = 3.5 + 0.1i. In this case, the underlying optical response of the system is isotropic and we do not expect material-inherent directionality for the emission. Possible directionality of the emission is instead caused by the interference of light in the nanostructure. To describe a spherically emitting dipole, that is, a dipole that emits inherently without directionality, we use a dipole moment density $\mathbf{P}_{dip} = P_{dip,x}\hat{\mathbf{e}}_x + P_{dip,y}\hat{\mathbf{e}}_y + P_{dip,z}\hat{\mathbf{e}}_z$ with isotropic $P_{dip,x} = P_{dip,y} = P_{dip,z} \equiv P_{dip}$.

We assume that the dipole occupies an infinitesimal volume dV around its center position $\mathbf{r}$ and emits in an infinitesimal wavelength range $d\lambda$ centered around λ. In this case, the rate of photons emitted to the top and the bottom side is given by [13]:

$$d\tilde{n}_{\mathrm{dip,TE(TM),top(bot)}}(\mathbf{r}) = 2\pi P_{\mathrm{dip}}(\lambda) n_{\mathrm{top(bot)}} d\lambda dV \times \int_0^{\pi/2} E^2_{\mathrm{enh,top(bot),TE(TM)}}(\mathbf{r}, \theta_{\mathrm{top(bot)}}) \sin(\theta_{\mathrm{top(bot)}}) d\theta_{\mathrm{top(bot)}}. \quad (2)$$

Here, we chose to include a prefactor to $P_{dip}(\lambda)$ such that $P_{dip}(\lambda)$ has the required units [$m^{-3}s^{-1}m^{-1}$] to yield the unit of [s^{-1}] to $d\tilde{n}_{dip,TE(TM),top(bot)}$. Importantly, in Eq. (2) we find the term $E^2_{enh,top(bot),TE(TM)}(\mathbf{r},\theta_{top(bot)}) = \frac{|\mathbf{E}_{loc,top(bot),TE(TM)}(\mathbf{r},\theta_{top(bot)})|^2}{|\mathbf{E}_{inc,top(bot),TE(TM)}(\theta_{top(bot)})|^2}$. This factor is the local field enhancement, which originates from the Lorentz reciprocity [13]. In more detail, the electric field of the dipole emission in a direction $\theta_{top(bot)}$ is reciprocal to the electric field $|\mathbf{E}_{loc,top(bot),TE(TM)}(\mathbf{r},\theta_{top(bot)})|$, which an incoming plane wave from direction $\theta_{top(bot)}$ of intensity $|\mathbf{E}_{inc,top(bot),TE(TM)}(\theta_{top(bot)})|$ causes at the location of the dipole [13]. Since the intensity is proportional to the refractive index and the electric field squared, $n_{top(bot)}E^2_{enh,top(bot),TE(TM)}(\mathbf{r},\theta_{top(bot)})$ is proportional to the emitted intensity in direction $\theta_{top(bot)}$ and hence enters Eq. (2). In order to calculate E_{enh}, we used the scattering matrix method [15] to calculate for varying incidence angle the electric field E_{loc} at the dipole position.

We study the emission of a dipole located at the top (z = 0), middle (z = L/2), and bottom (z = L) of the thin film (Fig. 2). Also here, we present polarization averaged results. Similarly as for the blackbody radiation above, we normalize the emission with the emission in a homogenous n = 3.5 surrounding.

The dipole located at the top of the thin film, that is, closest to the top n_{top} = 1.0 side, emits less and less light to the bottom side with increasing L (Fig. 2(a)). This decrease originates from the re-absorption of the emitted light inside the thin film before it reaches the bottom side. We note also that for small L, this dipole emits much stronger into the high-refractive index bottom side.

For the dipole placed in the middle of the thin film, the emission to both the top and the bottom side goes toward zero with increasing L (Fig. 2(b)). In this case of $L \to \infty$, emitted photons are re-absorbed before contributing to emission out from the thin film.

Finally, for the dipole at the bottom of the film, closest to the n_{bot} = 3.5 side, we find that light emitted toward the top side is re-absorbed more and more with increasing L (Fig. 2(c)). Furthermore, the emission to the bottom side settles to a value of 0.86 times the emission in the homogenous n = 3.5 surrounding. Here, this decrease is expected because of the reflection at the interface between the film with n_{film} = 3.5 + i0.1 and the bottom side with n_{bot} = 3.5, which goes toward 100% when $\theta_{bot} \to 90^0$ where the $\sin(\theta_{bot})$ factor in Eq. (2), due to the integration over the solid angle, gives the largest contribution to the emission.

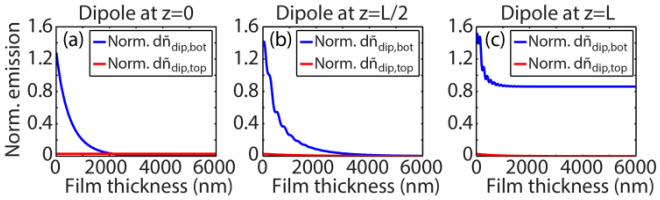

Fig. 2. Emission rate from a dipole located at (a) z = 0, (b) z= L/2, and (c) z = L in the thin film in Fig. 1(a). Here, we show both $d\tilde{n}_{dip,top}$ and $d\tilde{n}_{dip,bot}$, the emission rate to the top n_{top} = 1.0 side and to the bottom n_{bot} = 3.5 side, respectively. The emission is normalized to the emission from a dipole in a homogeneous n = 3.5 refractive index surrounding.

Above we saw how we could model both the blackbody radiation and the dipole emission of the thin film system. However, the blackbody radiation shows an explicit dependence on $(n_{top(bot)})^2$ [Eq. (1)] whereas the dipole emission shows a dependence on $n_{top(bot)}$ to the first power [Eq. (2)]. However, with the Lorentz reciprocity and the Kirchoff's reciprocity we can show the connection between these two types of light emission modeling.

We perform the analysis for a general three-dimensional nanostructure. We allow for a φ dependence of the emission, in addition to the θ dependence of the thin film above. Then, the dipole emission in Eq. (2) generalizes, including λ dependence, to

$$d\tilde{n}_{\mathrm{dip,TE(TM),top(bot)}}(\mathbf{r},\lambda) = P_{\mathrm{dip,gen}}(\mathbf{r},\lambda) n_{\mathrm{top(bot)}}(\lambda) \times d\lambda \int_0^{2\pi} d\phi_{\mathrm{top(bot)}} \int_0^{\pi/2} E^2_{\mathrm{enh,top(bot),TE(TM)}}(\mathbf{r},\lambda,\theta_{\mathrm{top(bot)}},\phi_{\mathrm{top(bot)}}) \times \sin(\theta_{\mathrm{top(bot)}}) d\theta_{\mathrm{top(bot)}}. \quad (3)$$

Here, we use $P_{dip,gen}(\mathbf{r},\lambda)$ to denote the dipole moment density in this general case. Note that we find in Eq. (3) the term

$$E^2_{\mathrm{enh,top(bot),TE(TM)}}(\mathbf{r},\lambda,\theta_{\mathrm{top(bot)}},\phi_{\mathrm{top(bot)}}) = \frac{|\mathbf{E}_{\mathrm{loc,top(bot),TE(TM)}}(\mathbf{r},\lambda,\theta_{\mathrm{top(bot)}},\phi_{\mathrm{top(bot)}})|^2}{|\mathbf{E}_{\mathrm{inc,top(bot),TE(TM)}}(\lambda,\theta_{\mathrm{top(bot)}},\phi_{\mathrm{top(bot)}})|^2}. \quad (4)$$

Similarly as above for the thin film, this local field enhancement factor originates from the Lorentz reciprocity [13]. This factor shows how much the emission into a specific direction is enhanced by interference effects in the nanostructure. It includes $|\mathbf{E}_{loc,top(bot),TE(TM)}(\mathbf{r},\lambda,\theta_{top(bot)},\varphi_{top(bot)})|$, the electric field intensity at the location $\mathbf{r}$ of the dipole due to $|\mathbf{E}_{inc,top(bot),TE(TM)}(\lambda,\theta_{top(bot)},\varphi_{top(bot)})|$, the electric field intensity of a TE(TM) polarized incident plane wave from polar angle $\theta_{top(bot)}$ and azimuth angle $\varphi_{top(bot)}$ from the top (bottom) side.

The blackbody radiation is in turn given by

$$d\tilde{n}_{\mathrm{BB,TE(TM),top(bot)}}(\lambda)=\frac{c\left(n_{\mathrm{top(bot)}}(\lambda)\right)^2}{\lambda^4\left[\exp(\hbar 2\pi c/(\lambda k_{\mathrm{B}}T))-1\right]} \quad (5)$$
$$\times d\lambda\int_0^{2\pi}d\phi_{\mathrm{top(bot)}}\int_0^{\pi/2}d\theta_{\mathrm{top(bot)}}A_{\mathrm{TE(TM),top(bot)}}(\lambda,\theta_{\mathrm{top(bot)}},\phi_{\mathrm{top(bot)}})\times\cos(\theta_{\mathrm{top(bot)}})\sin(\theta_{\mathrm{top(bot)}}).$$

To find the connection between these two emission types, we use that the absorbed power (Ohmic heating) for light incident from a direction given by $\theta_{\mathrm{top(bot)}}$ and $\varphi_{\mathrm{top(bot)}}$ is (see Eq. (3) in [16]):

$$dP_{abs,top(bot),TE(TM)}(\lambda,\theta_{top(bot)},\phi_{top(bot)})= \quad (6)$$
$$=d\lambda\int_{V_{structure}}\frac{2\pi c}{\lambda}\varepsilon_0\,\mathrm{Re}(n(\mathbf{r},\lambda))\,\mathrm{Im}(n(\mathbf{r},\lambda))\times E_{\mathrm{loc,TE(TM)}}(\mathbf{r},\lambda,\theta_{\mathrm{top(bot)}},\phi_{\mathrm{top(bot)}})^2\,dV.$$

Here, $V_{\mathrm{structure}}$ is the volume of the nanostructure. Specifically, notice that $n(\mathbf{r},\lambda)$ can show spatial dependence inside the nanostructure. Such spatial dependence allows the nanostructure to consist of several different materials. The incident intensity is given by

$$dP_{\mathrm{inc,top(bot)}}(\lambda,\theta_{\mathrm{top(bot)}},\phi_{\mathrm{top(bot)}})= \quad (7)$$
$$=d\lambda\int_{A_{\mathrm{structure}}}\frac{n_{\mathrm{top(bot)}}(\lambda)c\varepsilon_0}{2}\cos\left(\theta_{\mathrm{top(bot)}}\right)\times E^2_{\mathrm{inc,top(bot),TE(TM)}}(\lambda,\theta_{\mathrm{top(bot)}},\phi_{\mathrm{top(bot)}})dA.$$

where $A_{\mathrm{structure}}$ is the area of the nanostructure. Next, we employ that the absorptance is given by $A = \mathrm{d}P_{\mathrm{abs}}/\mathrm{d}P_{\mathrm{inc}}$. We obtain then, by using Eqs. (6)-(7) in Eq (5), that

$$d\tilde{n}_{\mathrm{BB,TE(TM),top(bot)}}(\lambda)= \quad (8)$$
$$=\int_{V_{\mathrm{structure}}}\left(\begin{array}{l}d\lambda\,\dfrac{4\pi c\,\mathrm{Re}(n(\mathbf{r},\lambda))\,\mathrm{Im}(n(\mathbf{r},\lambda))}{\lambda^5\left[\exp(\hbar 2\pi c/(\lambda k_{\mathrm{B}}T))-1\right]}\,n_{\mathrm{top(bot)}}(\lambda)\\ \times\displaystyle\int_o^{2\pi}d\phi_{\mathrm{top(bot)}}\int_0^{\pi/2}E^2_{\mathrm{enh,top(bot),TE(TM)}}(\mathbf{r},\lambda,\theta_{\mathrm{top(bot)}},\phi_{\mathrm{top(bot)}})\times\sin(\theta_{\mathrm{top(bot)}})d\theta_{\mathrm{top(bot)}}\end{array}\right)dV.$$

By comparing this equation to Eq. (3), we see that the choice

$$P_{\mathrm{dip,gen}}(\mathbf{r},\lambda)=\frac{4\pi c\,\mathrm{Re}(n(\mathbf{r}))\,\mathrm{Im}(n(\mathbf{r}))}{\lambda^5\left[\exp(\hbar 2\pi c/(\lambda k_{\mathrm{B}}T))-1\right]} \quad (9)$$

in Eq. (3) gives equivalency between the dipole emission and blackbody radiation, when the dipole emission is integrated over dipoles homogenously distributed through the volume of the nanostructure. Note that we by the use of this integration assume that the emission rate of one dipole does not depend on the existence of the other emitting dipoles in the nanostructure.

To show this correspondence in our numerical analysis of the thin film, we chose P_{dip} in Eq. (2) according to Eq. (9) and integrated over dipoles homogenously distributed throughout the volume of the thin film (see results marked by squares in Fig. 1(c)). As expected from Eqs. (3)–(9), we find perfect agreement with the results from the blackbody calculation (solid lines in Fig. 1(c)).

This description of blackbody radiation as emission from dipoles homogeneously distributed throughout the structure holds separately also for each polarization and emission direction. Furthermore, through this analysis, the apparent different dependence on $n_{\mathrm{top(bot)}}$ between the blackbody radiation [Eq. (1)] and dipole emission [Eq. (2)] has disappeared.

Finally, the dipole moment density $P_{\mathrm{dip,gen}}(\mathbf{r},\lambda)$ in Eq. (9) depends only on the material of the nanostructure at the location of the dipole, through its refractive index $n(\mathbf{r},\lambda)$. Thus, $P_{\mathrm{dip,gen}}$ is a material parameter that describes the inherent optical transitions resulting in emission in the absorbing material at a given wavelength and temperature. To support this conclusion on the meaning of $P_{\mathrm{dip,gen}}$, we used the $P_{\mathrm{dip,gen}}$ from Eq. (9) and assumed a homogenous surrounding, that is, $E_{\mathrm{enh}} = 1$ and $n_{\mathrm{top}} = n_{\mathrm{bot}} = N$, in Eq. (5). In this way, we obtained the same total photon emission rate $\mathrm{d}\tilde{n}_{\mathrm{dip}} = (\mathrm{d}\tilde{n}_{\mathrm{dip,TE.top}} + \mathrm{d}\tilde{n}_{\mathrm{dip,TM.top}} + \mathrm{d}\tilde{n}_{\mathrm{dip,TE.bot}} + \mathrm{d}\tilde{n}_{\mathrm{dip,TM.bot}})$ as with well-known results for photons emission in a homogenous semiconductor (see Eq. (10) in Ref. [17]). However, very importantly, our results, derived with the Kirchoff's and Lorentz' reciprocity, show that this dipole moment density applies also for nanostructures where interference effects can be substantial.

In conclusion, we showed how the results from modeling of blackbody radiation and dipole emission in a nanostructure can be compared. We can obtain equivalent results from both types of modeling if we choose the dipole moment density according to Eq. (9) and integrate the dipole emission over dipoles distributed throughout the nanostructure. However, note that for comparable results and physics, we need to make sure to use the same refractive index for both types of modeling. Specifically, $\mathrm{Im}(n) > 0$, which gives rise to $e > 0$ in blackbody emission modeling, must be included in the modeling of the dipole emission. Such $\mathrm{Im}(n) > 0$ introduces re-absorption of photons in the modeling of the dipole emission.

Funding. This work was supported by NanoLund, the Swedish Research Council (VR), the Swedish Foundation for Strategic Research (SSF), and the European Union's Horizon 2020 research and innovation programme under grant agreement No 641023, NanoTandem. This article reflects only the author's view and the Funding Agency is not responsible for any use that may be made of the information it contains.

References

1. W. Shockley, and H. J. Queisser, J. Appl. Phys. **32**, 510 (1961).
2. N. Anttu, ACS Photonics **2**, 446 (2015).
3. S. Sandhu, Z. F. Yu, and S. H. Fan, Opt. Express **21**, 1209 (2013).
4. Y. Xu, T. Gong, and J. N. Munday, Sci. Rep. **5**, 13536 (2015).
5. T. Tiedje, E. Yablonovitch, G. D. Cody, and B. G. Brooks, IEEE T. Electron. Dev. **31**, 711 (1984).
6. O. D. Miller, E. Yablonovitch, and S. R. Kurtz, IEEE J. Photovolt. **2**, 303 (2012).
7. E. D. Kosten, J. H. Atwater, J. Parsons, A. Polman, and H. A. Atwater, Light-Sci. Appl. **2**, e45 (2013).
8. L. Novotny, and B. Hecht, *Principles of Nano-Optics* (Cambridge University Press, 2012).
9. C. Wiesmann, K. Bergenek, N. Linder, and U. T. Schwarz, Laser Photon. Rev. **3**, 262 (2009).
10. P. D. Anderson, and M. L. Povinelli, Opt. Lett. **40**, 2672 (2015).
11. R. Paniagua-Dominguez, G. Grzela, J. G. Rivas, and J. A. Sanchez-Gil, Nanoscale **5**, 10582 (2013).
12. L. D. Landau, and E. M. Lifshitz, *Statistical Physics* (Elsevier Science, 2013).
13. J. Mertz, J. Opt. Soc. Am. B **17**, 1906 (2000).
14. A. I. Volokitin, and B. N. J. Persson, Rev. Mod. Phys. **79**, 1291 (2007).
15. N. Anttu, and H. Q. Xu, Phys. Rev. B **83**, 165431 (2011).
16. N. Anttu, Opt. Lett. **38**, 730 (2013).
17. G. Lasher, and F. Stern, Phys. Rev. **133**, A553 (1964).

1. W. Shockley, and H. J. Queisser, "Detailed Balance Limit of Efficiency of p-n Junction Solar Cells," J. Appl. Phys. **32**, 510-519 (1961).
2. N. Anttu, "Shockley-Queisser Detailed Balance Efficiency Limit for Nanowire Solar Cells," ACS Photonics **2**, 446-453 (2015).
3. S. Sandhu, Z. F. Yu, and S. H. Fan, "Detailed Balance Analysis of Nanophotonic Solar Cells," Opt. Express **21**, 1209-1217 (2013).
4. Y. Xu, T. Gong, and J. N. Munday, "The Generalized Shockley-Queisser Limit for Nanostructured Solar Cells," Sci. Rep. **5**, 13536 (2015).
5. T. Tiedje, E. Yablonovitch, G. D. Cody, and B. G. Brooks, "Limiting Efficiency of Silicon Solar-Cells," IEEE T. Electron. Dev. **31**, 711-716 (1984).
6. O. D. Miller, E. Yablonovitch, and S. R. Kurtz, "Strong Internal and External Luminescence as Solar Cells Approach the Shockley-Queisser Limit," IEEE J. Photovolt. **2**, 303-311 (2012).
7. E. D. Kosten, J. H. Atwater, J. Parsons, A. Polman, and H. A. Atwater, "Highly Efficient GaAs Solar Cells by Limiting Light Emission Angle," Light-Sci. Appl. **2**, e45 (2013).
8. L. Novotny, and B. Hecht, *Principles of Nano-Optics* (Cambridge University Press, 2012).
9. C. Wiesmann, K. Bergenek, N. Linder, and U. T. Schwarz, "Photonic Crystal LEDs – Designing Light Extraction," Laser Photon. Rev. **3**, 262-286 (2009).
10. P. D. Anderson, and M. L. Povinelli, "Optimized Emission in Nanorod Arrays through Quasi-Aperiodic Inverse Design," Opt. Lett. **40**, 2672-2675 (2015).
11. R. Paniagua-Dominguez, G. Grzela, J. G. Rivas, and J. A. Sanchez-Gil, "Enhanced and Directional Emission of Semiconductor Nanowires Tailored through Leaky/Guided Modes," Nanoscale **5**, 10582-10590 (2013).
12. L. D. Landau, and E. M. Lifshitz, *Statistical Physics* (Elsevier Science, 2013).
13. J. Mertz, "Radiative Absorption, Fluorescence, and Scattering of a Classical Dipole near a Lossless Interface: a Unified Description," J. Opt. Soc. Am. B **17**, 1906-1913 (2000).
14. A. I. Volokitin, and B. N. J. Persson, "Near-field radiative heat transfer and noncontact friction," Rev. Mod. Phys. **79**, 1291-1329 (2007).
15. N. Anttu, and H. Q. Xu, "Scattering Matrix Method for Optical Excitation of Surface Plasmons in Metal Films with Periodic Arrays of Subwavelength Holes," Phys. Rev. B **83**, 165431 (2011).
16. N. Anttu, "Geometrical optics, electrostatics, and nanophotonic resonances in absorbing nanowire arrays," Opt. Lett. **38**, 730-732 (2013).
17. G. Lasher, and F. Stern, "Spontaneous and Stimulated Recombination Radiation in Semiconductors," Phys. Rev. **133**, A553-A563 (1964).